Journal of Applied Electrochemistry **32**: 1011–1017, 2002.

Anode materials for lithium ion batteries from mild oxidation of natural graphite

Y.P. WU[1,2,*], C. JIANG[1], C. WAN[1] and R. HOLZE[2,*]
[1]*Division of Chemical Engineering, INET, Tsinghua University, Beijing 102201, China*
[2]*Technische Universität Chemnitz, Institut für Chemie, AG Elektrochemie, D-09107 Chemnitz, Germany*
*(*authors for correspondence: e-mail: wuyp99@hotmail.com; rudolf.holze@chemie.tu-chemnitz.de)*

Received 13 November 2001; accepted in revised form 6 June 2002

Key words: anode materials, graphite, lithium ion battery, mild oxidation

Abstract

Mild oxidation of a natural graphite in an ammonium peroxydisulfate solution yields promising anode materials. X-ray photoelectron spectroscopy, FTIR spectroscopy, electron paramagnetic resonance, thermogravimmetry, differential thermal analysis, high resolution electron microscopy and surface area measurements provided results suggesting that oxidation eliminates some reactive structural defects in this graphite. In addition, the surface of natural graphite is recoated with a dense layer of oxides forming an effective passivating film to prevent the decomposition of electrolyte and the movement of graphene molecules along its *a*-axis. Consequently, its thermostability and the EPR signal increase. In addition, the numbers of nanosized pores and channels increases, which provide more inlets and outlets for lithium intercalation and deintercalation and more sites for lithium storage. As a result, the reversible lithium capacity and the coulombic efficiency in the first cycle increase significantly and the cycling behaviour improves markedly. The reproducibility of product properties can be well controlled, and this method is promising for industry.

1. Introduction

Current research on anode materials for lithium ion batteries is very wide including graphitic carbons prepared at high temperatures (>2000 °C), amorphous carbons prepared at low temperatures (<1200 °C), nitrides, tin oxides and novel alloys [1, 2]. Recently, modification of graphite, especially surface modifications, has become an interesting topic. For example coating with various kinds of pyrolytic carbons [2–5], dipping in polymer solutions [6] or formation of dense oxide layers by oxidation with air, oxygen and carbon dioxide [7–11] provided significant improvements. The main weakness of graphitic materials is the presence of active sites at the graphite surface, some of which are defects. When they are moved or covered the surface of the electrode will not be so active, irreversible capacity will decrease and lithium intercalation is favored.

There are numerous kinds of graphitic carbons. Differences in source, treatment and processing result in striking differences in the surface and the body structure, let alone in the electrochemical performance as anode materials for lithium ion batteries. Recently, we investigated one kind of natural graphite from China [12]. Its reversible capacity was low, about 250 mAh g^{-1}, and cycling behaviour very poor. Its capacity faded to 100 mAh g^{-1} within 10 cycles, which is surprisingly different from data obtained with other natural or synthetic graphites [13, 14]. However, after catalytic oxidation, in which deposited metals acted as catalysts for the oxidation, its reversible capacity increased and its cycling behaviour improved. The reversible capacity was >372 mAh g^{-1}, that is the theoretical value of graphite [9]. It is, known that it is difficult to control the homogeneity and reproducibility of products of gas–solid interface oxidation reactions. Consequently, an oxidation reaction in the liquid phase is generally preferred [14]. Recently, we have tried aqueous solutions of H_2O_2 and $Ce(SO_4)_2$ as green oxidants and found a markedly improved electrochemical performance of the oxidized natural graphite from China [15]. The reduction potentials for H_2O_2/H_2O ($E_0 = 1.78$ V) and Ce^{4+}/Ce^{3+} ($E_0 = 1.61$ V) are lower than that of $S_2O_8^{2-}/SO_4^{2-}$ ($E_0 = 2.08$ V). Thus it is fair to consider a solution of ammonium peroxydisulfate, $(NH_4)_2S_2O_8$, as an effective oxidant. Here we report results obtained with this oxidant. Results differ significantly from those reported elsewhere [14]; our investigations provide detailed insight into the action of this mild oxidant. As is well known a change in surface structure alone could not result in striking enhancement of the reversible capacity, thus we provide detailed information on the action of the chemical oxidant beyond superficial changes.

2. Experimental details

A natural graphite from China (designated as D) with d_{002} 3.351 Å and L_c 120 Å was dipped into an aqueous solution 0.1 mol l^{-1} of $(NH_4)_2S_2O_8$ and 1 mol l^{-1} of H_2SO_4 at $T = 20$, 60, 100 and 120 °C, respectively, for some time, washed with water until the eluent was neutral and dried. The prepared products were designated as LS1, LS2, LS3 and LS4, respectively. X-ray photoelectron spectra (XPS) were obtained with an ES-300 spectrometer (Kratos, Japan). The relative contents of O and C at the surface of the natural graphite were calculated on the basis of their photoionization cross sections and the integrals of their X-ray photoelectron intensities. Electron paramagnetic resonance spectra (EPR) were acquired with an EPR-200 spectrometer (Bruker, Germany). Thermogravimmetry and differential thermal analysis (TG-DTA) were performed with an instrument PCT-1 under air (Beijing Analytical Instruments Co., China); the heating rate was 20 °C min^{-1}. High resolution electron micrographs (HREM) were recorded with a JEM-200CX microscope (Jeol, Japan). Samples were uniformly predispersed on micronets with cavities of μm size. FTIR spectra were obtained with a Nicolet 560 spectrometer with samples dried under vacuum prior to the measurement (Thermo Electron, USA). BET surface areas were measured with an ST-03 instrument through nitrogen sorption and desorption (Beijing Analytical Instruments Co., China). Distribution of particle (DPA) sizes was obtained with a SA-CP3 particle size analyzer (Shimadzu, Australia/New Zealand), and the outer specific surface areas were calculated assuming that the particles were spherical. Capacity and cycling behaviour were tested by the method reported elsewhere [15], which used lithium foil as the counter and reference electrode and a solution of 1 mol l^{-1} $LiClO_4$ in a mixture of EC/DEC (v/v = 3:7) as electrolyte and a homemade porous PP film as separator. The anode was prepared by pressing the mixture of natural graphite and 5 wt.% binder PVDF dissolved in *N*,*N*′-dimethylformamide into pellets with a diameter of about 1 cm. After drying under vacuum at 120 °C overnight, the anode pellets were put into an argon box and assembled into model cells. Electrochemical performance was measured galvanostatically at 0.2 mA with a CT2001A cell test instrument (Wuhan Land Electronic Co., China), discharge (intercalation process) and charge (deintercalation process) voltage was ranged from 0.0 to 2.0 V vs Li^+/Li.

3. Results and discussion

The oxidation capability of $(NH_4)_2S_2O_8$ is the strongest among the compounds stable in aqueous solutions. It is known that there are many structural imperfections such as sp^3-hybridized carbon atoms, edge carbon atoms and carbon chains in graphite [16, 17], especially in natural graphite, due to its incomplete graphitization during the natural formation process. These kinds of structures are prone to oxidative removal during reaction with a solution of $(NH_4)_2S_2O_8$. Consequently, the surface structure of the natural graphite D will change during oxidation. XPS spectra of O_{1s} in the samples D and LS2 are shown in Figure 1 and selected results are summarized in Table 1. They indicate that oxygen atoms are present in four kinds of species before and after oxidation, that is, hydroxyl/phenolic oxygen, ether oxygen, carboxylic oxygen in –COOR (R = H and alkyl) and carbonyl oxygen in acetone/quinone, which correspond to binding energy peaks at 534.1, 533.2, 532.3 and 530.9 eV, respectively [18, 19].

X-ray photoelectron spectra of C_{1s} in the samples D and LS2 are shown in Figure 2, selected data are also summarized in Table 1. Four kinds of carbon atoms species are present, that is, carbonyl carbon in acetone/quinone, carboxylic carbon in –COOR (R = H and alkyl), ether/phenolic carbon in C–O–C and C–OH, and carbon atoms in graphene planes, which correspond to binding energies at 288.9, 287.2, 285.9 and 284.4 eV, respectively [18, 19]. In the case of natural graphite before the oxidation treatment, it is known that it chemisorbs and/or physisorbs oxides such as water, oxygen and CO_2. The graphite employed here was treated in KOH solution to remove minerals. Four kinds of oxides were also observed like with samples from oxidation [20]. However, we could not obtain sufficient evidence indicating which kind(s) of compound(s)

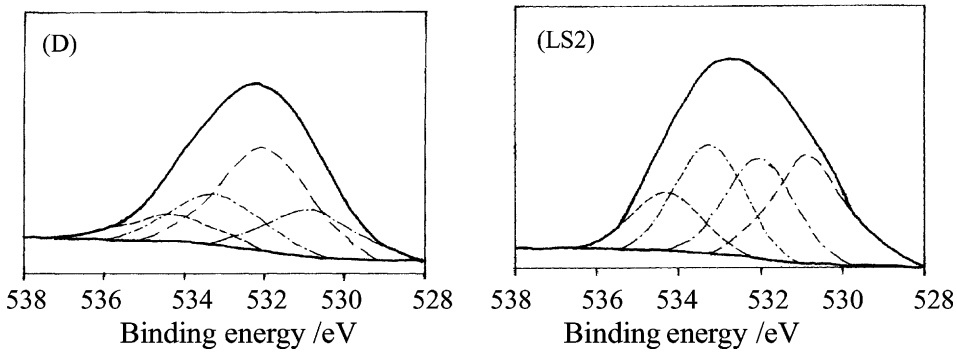

Fig. 1. XPS spectra of O_{1s} at the surface of natural graphite before (D) and after oxidation treatment (LS2).

Table 1. Experimental data of the natural graphite before (D) and after (LS1, LS2, LS3 and LS4) oxidation with a solution of $(NH_4)_2S_2O_8$

Sample	Treatment temperature /°C	Weight loss /%	Atomic ratio of O at the surface /%	Atomic ratio of C at the surface /%	Species and contents of oxygen atoms				Species and contents of carbon atoms			
					534.1 eV	533.2 eV	532.3 eV	530.9 eV	288.9 eV	287.2 eV	285.9 eV	284.4 eV
D	–	–	4.11	95.89	0.1268	0.2320	0.4526	0.1886	0.0299	0.0534	0.1029	0.8138
LS1	20	2.64	4.70	95.30	0.1563	0.2651	0.3242	0.2544	0.0367	0.0575	0.0837	0.8221
LS2	60	2.07	6.03	93.97	0.1538	0.2834	0.2563	0.3065	0.0353	0.0641	0.1449	0.7556
LS3	100	1.83	5.95	94.05	0.1020	0.2800	0.3933	0.2247	0.0337	0.0441	0.0973	0.8249
LS4	120	1.67	5.33	94.67	0.1621	0.3251	0.3567	0.1560	0.0300	0.0717	0.1396	0.7587

was(were) involved preferably by oxidation with $(NH_4)_2S_2O_8$. One reason is that the oxidation reaction was complicated. Perhaps the acetone/quinone groups and ether/phenol were mainly changed since their relative content increased, seen from the changes in the relative contributions of the peaks at 533.2 and 288.9 eV.

Certainly, weakly adsorbed oxygen atoms were removed and replaced by a layer of oxides, from the oxidation, bonded more firmly to the carbon structure [21] because results in Table 1 show that the content of oxygen atoms at the surface increased from 4.11 to 4.70, 6.03, 5.95 and 5.33%, and there was a slight weight loss after the mild oxidation treatment, 2.64, 2.07, 1.83 and 1.67%. In previous experiments [15] we tried to reoxidize an oxidized natural graphite. We found that the weight loss was much less than that during the first treatment, which clearly indicated that the active structural imperfections such as sp^3-hybridized carbon atoms, edge carbon atoms and carbon chains existed in the natural graphite and some of them were removed during the above oxidation treatment, though the amounts were small. No method has been found to determine them precisely.

FTIR spectra of oxidized natural graphite LS2 were obtained using natural graphite D as the reference sample (Figure 3). Some surface oxygen-including groups were apparently identified, which is consistent with the results from XPS, in particular the increase in surface oxygen content. A few absorption bands are identified. A very strong band centered at 3451 cm^{-1} is assigned to $\nu_{(O-H)}$ of alcoholic/phenolic groups. The band at 1741 cm^{-1} is characteristic of the stretching band of carbonyl groups, $\nu_{(C=O)}$, and that at 1637 cm^{-1} is due to $\nu_{(C=O)}$ of quinone [2]. The band at 1371 cm^{-1} may be assigned to $\delta_{(O-H)i.p.}$ of alcoholic phenolic groups. Around 1000 cm^{-1} there is a wide, weak band corresponding to $\nu_{as(C-O-C)}$ in ether.

EPR spectra of natural graphite of D and LS2 are shown in Figure 4. The concentration of free spins increased greatly, from 9.79×10^{11} g^{-1} (D) to 2.87×10^{12} g^{-1} (LS2). This, apparently, resulted from mild oxidation, which eliminated some active structural defects such as carbon chains and sp^3-hybridized carbon atoms and produced radicals. Of course, if these kinds of radicals were situated at the surface of natural graphite, they would deactivate very quickly and we could not observe these radicals. It is assumed that these kinds of radicals are situated inside of natural graphite since the $\bullet HSO_4^-$ radical ion can penetrate into the graphene layers. Consequently, the radicals were stable and could be detected. This is evidently different from experiments that used air as an oxidation agent for the high purity NG-7 graphite [10]. In the latter case, it was found that the EPR intensity decreased sharply.

Since some reactive structural imperfections were eliminated, the structure of the prepared natural graphite became more stable. Curves of thermogravimmetry and differential thermal analysis (TG-DTA) of D and

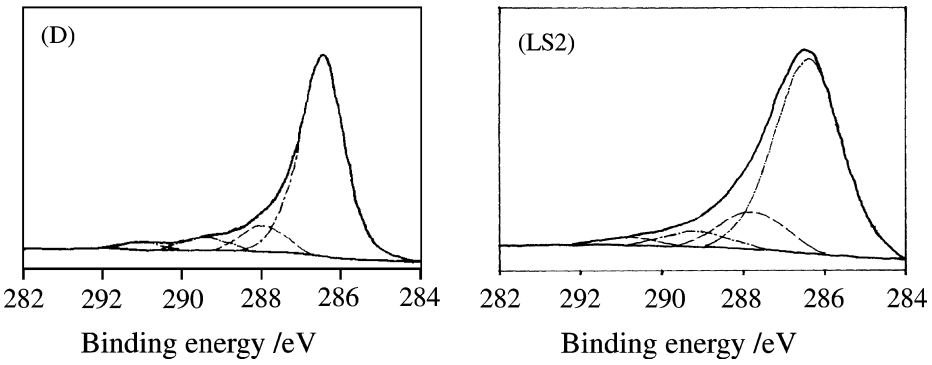

Fig. 2. XPS spectra of C_{1s} at the surface of natural graphite before (D) and after oxidation treatment (LS2).

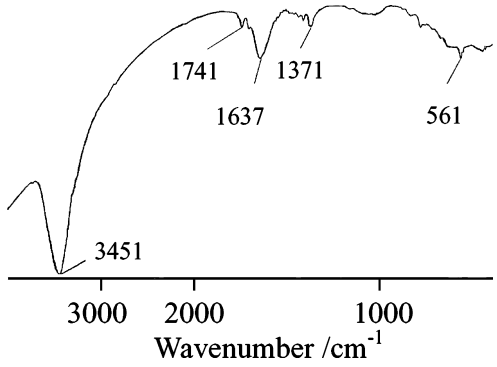

Fig. 3. FTIR spectrum of the prepared natural graphite LS2 using natural graphite D as the reference sample.

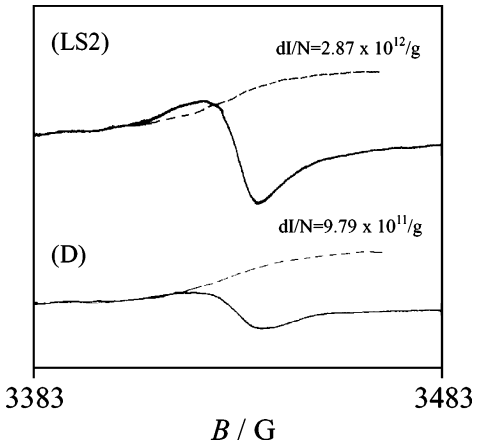

Fig. 4. EPR spectra of natural graphite before (D) and after oxidation treatment (LS2) measured at room temperature.

the prepared natural graphite samples (LS1, LS2 and LS3) are shown in Figure 5. At first, the weight decreased slowly because of thermal decomposition of some oxides and slight oxidation. At temperatures above 500 °C, combustion began and the DTA curves increased. When the combustion reaction occurred rapidly, the DTA curves peaked. After the oxidation treatment of the graphite the exothermal peaks shifted from 742 to 761, 761 and 752 °C, respectively. Usually, defects are easily oxidized and initiate the combustion reaction of natural graphite at lower temperatures. After

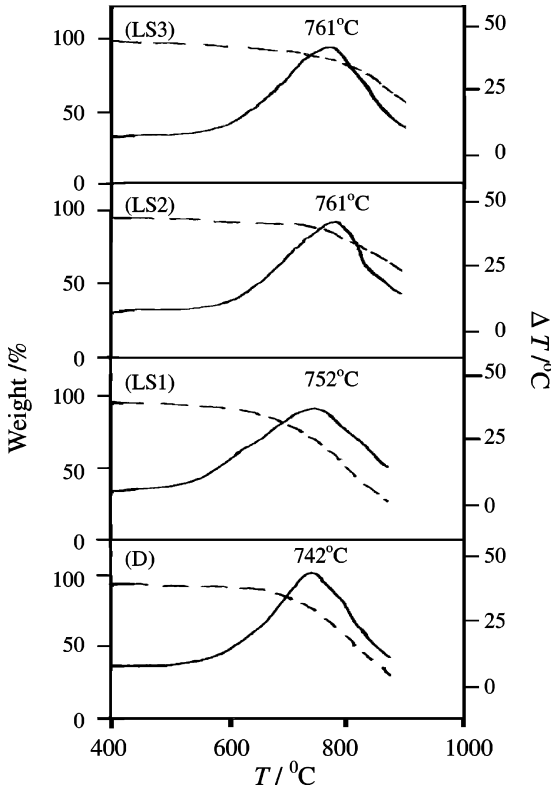

Fig. 5. TG-DTA curves of natural graphite before (D) and after (LS1, LS2, and LS3) oxidation treatment. Curves: (- - - -) TG; (—) DTA.

the removal of these active sites, the natural graphite structure became more stable, and the exothermal peaks shifted to higher temperatures, which is consistent with the discussion above, though the shift is small.

HREM micrographs of natural graphite D and LS1 are shown in Figure 6, and indicate an increase in the number of micropores and nanochannels after mild oxidation. This increase should be reflected in the surface area data. Results of BET measurement are summarized in Table 2. Surprisingly, the specific surface area determined with the BET-method is diminished after mild oxidation. Most likely small surface particles and reactive functional groups are oxidatively removed resulting in a 'smoother' surface. This seems to contradict, at first glance, the microscopic results, but both are evidently correct. Additional data on the distribution of

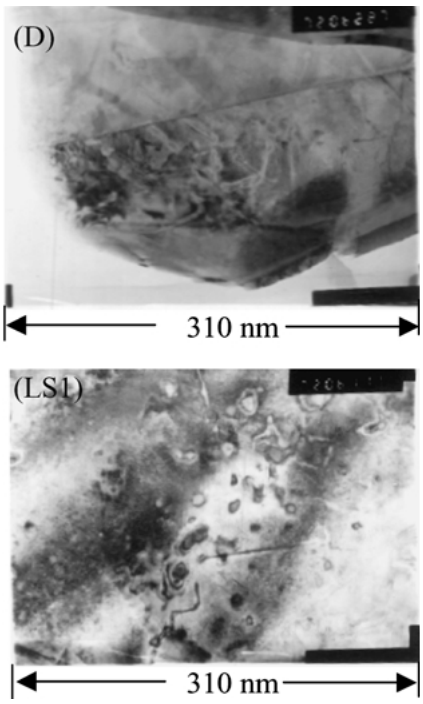

Fig. 6. HREM micrographs of natural graphite before (D) and after (LS1) oxidation treatment.

Table 2. BET data and outer surface area data based on distribution of particle diameter (DPA) of natural graphite before (D) and after (LS1 and LS2) the mild oxidation

Sample	Specific surface area from BET /$m^2\ g^{-1}$	Outer specific surface area from DPA /$m^2\ g^{-1}$	Calculated inner specific surface area /$m^2\ g^{-1}$
D	5.34	1.229	4.11
LS1	5.09	0.623	4.37
LS3	4.92	–	–

particle diameters of natural graphite D and LS1 were measured in order to clarify this apparent inconsistency. The outer specific surface area was calculated assuming spherical particles and is included in Table 2. The calculation could not take into account the fact that natural graphite particles were not perfectly spherical, thus the values are somewhat uncertain. From the difference, the inner specific surface area can be calculated, as also listed in Table 2. This implies clearly that the internal surface area and, consequently, the number of micropores and nanochannels has increased during oxidation, which is also consistent with results from the oxidation of an activated carbon [21]. This results support the initial suggestion that results of the BET measurement reflect the total surface area, whereas HREM mainly images micropores, corresponding to the inner specific surface area. The total specific surface area, of course, includes the outer specific surface area that, in turn, has been obtained from the distribution of particle diameters.

Discharge and charge profiles of natural graphite D and the prepared samples LS1, LS2, LS3 and LS4 in the first cycle and discharge profiles in the second cycle are presented in Figure 7. As mentioned above, the electrochemical properties of the natural graphite without this treatment were poor and its reversible capacity was only 251 mAh g^{-1}. The reversible capacity is increased to >350 mAh g^{-1} after mild oxidation. As mentioned above, some reactive structural imperfections were eliminated, and therefore the decomposition of electrolyte solvent molecules such as EC and DEC was less likely. In addition, the surface of natural graphite was covered with a fresh and dense layer of oxides including hydroxyl/phenol, ether, ester and carbonyl groups. This layer could act as a passivating film when lithium intercalated, and also hindered the decomposition of solvent molecules and the cointercalation of solvated Li^+. Consequently, the irreversible capacity above 0.3 V in the first cycle decreased, and the coulombic efficiency in the first cycle increased from 64% to >85% after oxidation.

The enhancement of reversible capacity can be mainly ascribed to the increase in the number of micropores and nanochannels through the mild oxidation treatment and to the elimination of structural imperfections. It is well known that micropores can act as matrices for lithium storage in the form of lithium molecules or lithium clusters [22, 23]. In addition, micropores provide inlets and outlets for lithium during the discharge and charge process, and favour lithium intercalation.

The effects of radicals are not clear at present. However, since they must be located inside the graphite, they did not lead to evident side reactions. Their specific action with respect to lithium is under further study.

Cycling behaviour of natural graphite D and the prepared samples LS1, LS2 LS3 and LS4 is presented in Figure 8. In the case of natural graphite D, the reversible capacity faded to 100 mAh g^{-1} in the first 10 cycles. After mild oxidation, the cycling behaviour is considerably improved. In the case of LS1 and LS2 there was no evident fading of the reversible capacity. In the case of LS3 and LS4 there was a slight fading, but the

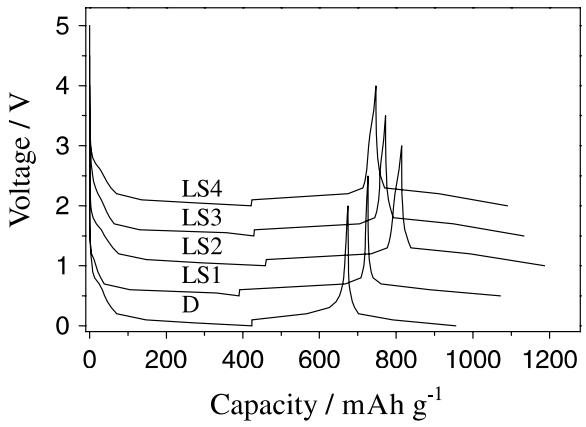

Fig. 7. Discharge and charge profiles of natural graphite before (D) and after (LS1, LS2, LS3 and LS4) mild oxidation by the $(NH_4)_2S_2O_8$ solution in the first 1.5 cycles (For clarity, voltages of LS1, LS2, LS3 and LS4 were shifted upwards by 0.5, 1.0, 1.5, and 2.0 V, respectively).

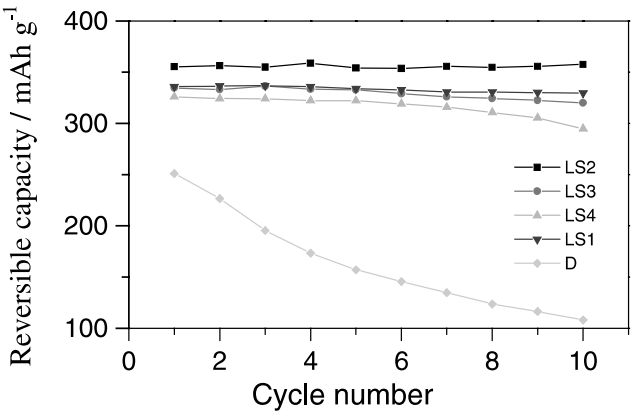

Fig. 8. Cycling behaviour of natural graphite before (D) and after (LS1, LS2, LS3 and LS4) mild oxidation by the $(NH_4)_2S_2O_8$ solution.

performance was still much better than that of natural graphite D. Results show that the stability of the natural graphite structure was improved and a dense layer of oxides was formed after mild oxidation with $(NH_4)_2S_2O_8$. Side reactions, such as cointercalation of solvated lithium ions and the movement of graphene planes around the *a*-axis, became hindered, which suggests that exfoliation or destruction of graphite became more difficult [15]. As a result, the graphite structural stability improves and reversibility for lithium intercalation and deintercalation is ensured. Consequently, the cycling behaviour of the modified natural graphite as anode material for lithium ion battery improved.

Figures 7 and 8 also suggest that improvement in electrochemical performance became less pronounced with oxidation temperatures above 60 °C. $(NH_4)_2S_2O_8$ will decompose quickly at temperatures above 60 °C, and thus not all the chemical oxidant participates in the oxidation reaction and the oxidation becomes less effective.

Based on the above suggested actions of the strong chemical oxidant $(NH_4)_2S_2O_8$ and our former results [15], other kinds of chemical oxidants such as HNO_3, $KClO_3$ and HClO can also be used to modify natural graphite. Results on the improved electrochemical performance of the obtained oxidized natural graphites as anode materials for lithium ion battery will be published elsewhere [24]. We have used other kinds of common natural graphite and the same striking improvement was also achieved [25].

In a pilot plant, we have tried this method on a larger scale. The electrochemical performance, including the capacity and the cycling of the assembled lithium ion battery, which used $LiCoO_2$ as cathode, was also very good.

4. Conclusion

Mild oxidation of natural graphite in a $(NH_4)_2S_2O_8$ solution can effectively improve its electrochemical performance as anode material for lithium ion batteries, the main reasons being due to the following factors:

(i) Some structural imperfections with high reactivities toward lithium ions such as carbon chains, edge carbon atoms and sp^3-hybridized carbon atoms are eliminated. The chemical reactivity of the surface decreases and the decomposition of electrolyte molecules is hindered.

(ii) More micropores and nanochannels are introduced, which act as matrices for lithium storage, and inlets and outlets for lithium intercalation and deintercalation.

(iii) The surface of natural graphite is modified and covered with a dense oxide layer, which results in an increase in the stability of the graphite structure, preventing the cointercalation of solvated lithium ions and the movement of graphene planes along its *a*-axis.

As a result, the reversible capacity increases from 251 to >350 mAh g^{-1}, the coulombic efficiency in the first cycle increases from 64% to >85%, and the reversible capacity does not appear to fade.

These results are different from those reported elsewhere [14], which only illustrated a change in the surface structure, though it was said that further studies were underway. One of the reasons leading to this striking difference is the choice of graphite. Ein-Eli and Koch used a high-grade synthetic graphite, whose reversible capacity was up to 370 mAh g^{-1} showing good cycling behaviour. In our case, only common natural graphite was used with inferior electrochemical performance, as stated above. The method of oxidation introduced here may be a promising method to manufacture anode materials for lithium ion batteries from common natural graphite under mild conditions and can be used to control the homogeneity of the products easily. In addition, the requirements for the primary material, natural graphite, are low.

Acknowledgement

Financial supports from China Postdoctor Foundation and Alexander von Humboldt Foundation are appreciated.

References

1. J.O. Besenhard (Ed.) 'Handbook of Battery Materials', (Wiley–VCH, Weinheim, 1999).
2. Y.P. Wu, C. Wan, C. Jiang and S.B. Fang, 'Principles, Introduction and Advances of lithium Secondary Batteries' (Tsinghua University Press, Beijing, 2002).
3. S. Yoon, H. Kim and S.M. Oh, *J. Power Sources* **94** (2001) 68.
4. Y. Kida, K. Yanagida, A. Funahashi, T. Nohma and I. Yonezu, *J. Power Sources* **94** (2001) 74.
5. H. Wang and M. Yoshio, *J. Power Sources* **93** (2001) 123.
6. M. Gaberek, M. Bele, J. Drofenik, R. Dominko and S. Pejovnik, *J. Power Sources* **97–98** (2001) 67.

7. E. Peled, C. Menachem and A. Melman, *J. Electrochem. Soc.* **143** (1996) L4.
8. T. Nakajima and K. Yanagida, *Tanso* **174** (1996) 195.
9. Y.P. Wu, C.Y. Jiang, C.R. Wan and E. Tsuchida, *Electrochem. Commun.* **2** (2000) 272.
10. C. Menachem, Y. Wang, J. Floners, E. Peled and S.G. Greenbaum, *J. Power Sources* **76** (1998) 180.
11. H. Buqa, P. Golob, M. Winter and J.O. Bensenhard, *J. Power Sources* **97–98** (2001) 122.
12. Y.P. Wu, C. Jiang, C. Wan and J. Li, *Battery* **30** (2000) 143.
13. T.D. Tran, J.H. Ferkert, X. Song and K. Kinoshita, *J. Electrochem. Soc.* **142** (1995) 3297.
14. Y. Ein-Eli and V.R. Koch, *J. Electrochem. Soc.* **144** (1997) 2968.
15. Y.P. Wu, C. Jiang, C. Wan and E. Tsuchida, *J. Mater. Chem.* **11** (2001) 1233.
16. L.C.F. Blackman, 'Modern Aspects of Graphite Technology' (Academic Press, London and New York, 1970).
17. G.C. Chung, S.H. Jun, K.Y. Lee and M.H. Kim, *J. Electrochem. Soc.* **146** (1999) 1664.
18. Z. Wu and C.U. Pittman, *Carbon* **33** (1995) 597.
19. U. Zielke, K.J. Huttinger and W.P. Hoffman, *Carbon* **34** (1996) 983.
20. C. Wong, R.T. Yang and B.L. Halpern, *J. Chem. Phys. 1* **78** (1983) 3325.
21. C. Moreno-Castilla, M.A. Ferro-Garcia, J.P. Joly, I. Bautista-Toledo, F. Carrasco-Marin and J. Rivera-Utrilla, *Langmuir* **11** (1995) 4386.
22. Y.P. Wu, C. Wan, C. Jiang, S.B. Fang and Y.Y. Jiang, *Carbon* **37** (1999) 1901.
23. A. Mabuchi, T. Katsuhisa, H. Fujimoto and T. Kasuh, *J. Electrochem. Soc.* **142** (1995) 1041.
24. Y.P. Wu, C. Jiang, C. Wan and R. Holze, *Solid State Ionics*, in press.
25. Y.P. Wu, unpublished results.